MEASUREMENT OF THE MINORITY CARRIER DIFFUSION LENGTH AND EDGE SURFACE-RECOMBINATION VELOCITY IN InP

Roshanak Hakimzadeh[1,2] and Sheila G. Bailey[3]

[1]Sverdrup Technology, Inc., Lewis Research Center Group, Brook Park, Ohio 44142

[2]Case Western Reserve University, Cleveland, Ohio 44106

[3]NASA Lewis Research Center, Cleveland, Ohio 44135

A scanning electron microscope (SEM) was used to measure the electron (minority carrier) diffusion length (L_n) and the edge surface-recombination velocity (V_s) in zinc-doped Czochralski-grown InP wafers. Electron-beam-induced current (EBIC) profiles were obtained in specimens containing a Schottky barrier perpendicular to the scanned (edge) surface. An independent technique was used to measure V_s, and these values were used in a theoretical expression (Donolato, Ref. 12) for normalized EBIC. A fit of the experimental data with this expression enabled us to determine L_n.

I. INTRODUCTION

The minority carrier diffusion length (L) is an important parameter in determining the performance of minority carrier devices, such as solar cells. In the past many different techniques have been used to determine L. Some rely on the measurement of the minority lifetime by means of photoluminescence [1,2]. The scanning electron microscope (SEM) is widely used for the measurement of L. With the SEM a high energy electron beam can be used in a line scan mode to generate a volume of charge carriers within the sample. The advantage of using an electron beam as opposed to other sources of excitation, such as optical [3], is that the volume and depth of generation can be accurately controlled by varying the beam voltage.

In the "normal collector geometry" the p-n junction or Schottky barrier is viewed edge-on. With the SEM in a line scan mode, the electron beam scans the semiconductor perpendicular to the potential barrier (Figure 1). The generated charge carriers can then diffuse to the potential barrier where the electrons and holes are separated and a current, I(x,z), is generated in the external circuit. This current, referred to as electron-beam-induced current (EBIC), reflects the

amount of excess carriers generated. The surface on which the beam impinges acts as a surface recombination path into which the generated minority carriers diffuse and are annihilated. We will refer to the recombination velocity of this surface as the edge-surface recombination velocity, V_s (cm/sec).

If we make the assumption that the electric field outside the junction space charge region is negligible, the transport of the generated minority carriers is purely diffusive. Under this condition, and if $V_s=0$, the EBIC will decrease exponentially with increasing distance, x, from the junction as follows:

$$I(x,z) = I(o)\exp(-\frac{x}{L})\Big|_{z\text{-const.}} \qquad (1)$$

(For a definition of the coordinate system refer to Figure 1.) A plot of log[I(x,z)] versus x, therefore, would result in a straight line from which L can be found. If the diffusion length is different on either side of the junction, the slopes will also be different. The plot will go through a peak which occurs at the metallurgical junction, as shown in Figure 2 [4]. In practice, however, V_s cannot be neglected and the plot of log [I(x,z)] versus x is no longer linear but appears concave upward near the junction, becoming steeper with increasing V_s.

Increasing the electron beam accelerating voltage, V_o, increases the depth at which the carriers are generated, thereby minimizing the effect of V_s. However, for large beam voltages the electron range, R, may become comparable to the value of L, diminishing the resolution of the technique [5]. Figure 3 shows a plot of R as a function of the beam voltage, V_o. Throughout this work V_o was limited to 15 KV.

Several theoretical expressions have been derived for the induced current profile which incorporate the effects of V_s. The first such expression was derived by Van Roosbroeck [6] from the solution of the diffusion problem for a point source of minority carriers at a depth, z, in a semi-infinite specimen. Other papers have been published which refer to Van Roosbroeck [7]. Expressions based on more realistic generation schemes, such as the uniform sphere or the spherically symmetric Gaussian, have also been derived [8-12]. These expressions give the induced current profile in terms of integrals of a modified Bessel function. In limiting cases ($V_s \to 0$, $V_s \to \infty$) these lead to analytical expressions of I(x,z) which have exact solutions. However, for arbitrary V_s, these have to be solved numerically.

Donolato derived a simpler expression for I(x,z) through the use of the Fourier transform method [13]. The simplification results from the consideration of a two-dimensional study of the diffusion problem. Hakimzadeh *et al.* [14] have measured the minority carrier diffusion length in GaAs solar cells by fitting experimentally obtained EBIC

profiles to Donolato's equation. In their study, an independent technique was used for the measurement of V_s as a function of x [15].

In this work we have applied the experimental technique described in [14] to measure electron diffusion length, L_n, in Zn-doped InP materials. A review of the theoretical approach is given in Section II.

II. REVIEW OF THE THEORY

The expression derived by Donolato is shown in Equation 2.

$$\frac{I(x,z)}{I(0,z)} = \frac{2}{\pi}\int_0^{\infty} \frac{K}{\mu^2}\left(\exp\left(-\frac{K^2\sigma^2}{2}\right) - 0.57\times\exp\left(\frac{\lambda^2\sigma^2}{2}-\mu Z_o\right)\right.$$
$$\left.\times\frac{s}{\mu+s}\,erfc\left[\frac{\sigma}{\sqrt{2}}\left(\mu-\frac{Z_o}{\sigma^2}\right)\right]\right)\times\sin(Kx)\,dK \qquad (2)$$

where:

$$\lambda = \frac{1}{L} \qquad (3)$$

$$\mu = (K^2+\lambda^2)^{\frac{1}{2}} \qquad (4)$$

$$\lambda = \frac{R}{\sqrt{15}} \qquad (5)$$

$$s = \frac{V_s}{D} \qquad (6)$$

where R is the range of the generation volume in μm, K is the wavenumber, D is the minority carrier diffusion coefficient in cm^2/sec, and I(0,z) is the maximum EBIC collected at the junction in amperes. If we assume the generation volume to be a three-dimensional Gaussian, the

range, R, will be given by [16]:

$$R = \frac{0.0276\, A V_o^{1.67}}{(Z^{0.889}\rho)} \quad \mu m \qquad (7)$$

where V_o is in KV, A is the atomic weight in g/mole, Z is the atomic number of the target, and ρ is the density of the semiconductor in g/cm^3. It can be seen that the two unknowns in Equation 2 are L and s.

The technique developed by Watanabe *et al.* [15] was used to measure s as a function of x. Their Equation is repeated here in our notation:

$$s = \frac{V_s}{D} = \frac{\partial}{\partial Z_o} \ln I(x,z) \Big|_{z_o=0} \qquad (8)$$

EBIC profiles were obtained along the same line scan for a number of accelerating voltages, from 4 KV to 15 KV. For each point, x, s was obtained from the slope of the ln[I(x,z)] versus Z_o plot using Equation 8. A typical plot is shown in Figure 4. The s values obtained in this manner were stored in an ASCII data file. The advantage of working with s rather than V_s is that D need not be known. This eliminates errors resulting from a calculated value of D.

To obtain L_n, EBIC profiles for a 15 KV accelerating voltage were used. A program was written in FORTRAN to perform the integration in Equation 2 by approximating the generation volume by a Gaussian. The accuracy of this program has been checked previously [14]. When running the FORTRAN program the user is prompted for V_o, I(0,z), the names of the ASCII data files containing experimentally obtained I(x,z) and the s values. I(0,z) was calculated by extrapolating the experimental plots of log[I(x,z)] versus x back to the junction, as described in [14]. The program calculates values of L_n for different points, x, and outputs these to an ASCII data file.

III. EXPERIMENTAL DETAILS

The aim of this work was to measure L_n in InP materials. For this reason Schottky barriers were formed to minimize the effect of processing which may result from junction formation. We used Czochralski-grown zinc-doped InP wafers with reported carrier densities of 2×10^{16} cm^{-3} and 1×10^{18} cm^{-3}, purchased from Crystacomm. All wafers were of (100) surface orientation with an uncertainty of 2° off axis towards (110). Ohmic contacts were evaporated on the back (unpolished) surface. Gold Schottky contacts (2000 Å thick) were evaporated on the front

(polished) surface in the form of 2.5 mm-diameter dots. The specimens were cleaved to expose the rectifying junction, as shown in Figure 5. SEM sample holders held these specimens in place and made electrical contacts to the front and back of the specimens. EBIC profiles were obtained by scanning the electron-beam along this cleaved edge, and the analysis was carried out as described in Section II.

We observed an unexpected effect which prevented us from measuring L_n in the lower doped materials. This effect and other results will be discussed in Section IV.

IV. RESULTS AND DISCUSSION

We found that in the lower doped specimens EBIC profiles did not decay very much with increasing x implying that charge collection occurs with approximate unity efficiency up to hundreds of micrometers from the Schottky barrier. An example is shown in Figure 6. This effect has been observed before in Si [17] and is thought to be due to an inversion layer which forms as a result of the interaction of the electron beam with the native oxide at the surface. The charge introduced by the electron beam on this surface is annihilated by the nearby holes and results in a negatively charged layer close to the surface. This inversion layer created near the surface results in the collection of the beam-generated minority carriers along the entire length of the scan.

In Si [17] it has been shown that after about 20 successive scans the charge collection efficiency at large distances from the junction is progressively reduced [17], and finally normal behavior is re-established. This was not observed here for InP, even after many more scans.

To alleviate this problem, we attempted to remove the native oxide prior to the SEM characterization by etching the edge surface in a solution of 10% HF [18]. However, even in the vacuum chamber of the SEM (which is ~ 10^{-5} or 10^{-6} Torr) we were unable to keep the oxide layer from building up long enough to make the necessary measurements.

This surface inversion effect was not observed in the higher-doped specimens since they require much more charge at the surface to create an inversion layer. EBIC profiles in these higher-doped specimens decayed with increasing x, as expected. The analysis described in Section II was applied to measure L_n and s as a function of x in these specimens. Typical results are shown in Figure 7.

Figure 7 illustrates that L_n increases sharply as the junction is approached. This is due to the fact that the lateral extension of the generation volume is $\varepsilon \sim 2\sigma \sim R/2$ [13], therefore Donolato's equation is only applicable for $x \geq R/2$. For $x < R/2$ the effect seen is an artifact since Donolato's equation no longer holds in this region. At large distances, x, L_n is seen to increase again. In these regions the

EBIC measured is very small and comparable in magnitude to the beam current. This results in a large error in the measured values of L_n. We therefore concentrate only in the middle regions where L_n appears to be constant. In these regions the measured values of L_n and s were as shown in Table I. These results are in the right ballpark as compared to previously published results which indicate that for p-type InP with a carrier concentration of 1 x 10^{18} cm^{-3} L_n is about 3 μm [19]. If we assume that D is a constant in these specimens and is approximately equal to 104 cm^2/sec, the measured V_s values ranged from 40.86 to 1.80 x 10^3 cm/sec.

The aim of this work was to measure the L_n values in the bulk. Therefore, it was necessary to ensure that the measured values were not in any way affected by surface defects. The edge surface of some typical samples were etched in concentrated HCl acid for about 15 seconds. This created a uniformly "pitted" surface as shown in Figure 8. It has been shown that etching in concentrated HCl for this length of time removes about 3 μm from this edge surface [20].

EBIC analysis was carried out on such treated samples, and L_n and s values were determined as described in Sections II and III. Figure 9 shows the results before and after treatment for a typical sample. It can be seen that although the s values have increased in the treated samples, L_n appears to remain constant.

REFERENCES

1. C.H. Wang, IEEE Trans. Electron Devices, **38** (9), 2169 (1991).

2. P. Jenkins, G.A. Landis, I. Weinberg and K. Lneisel, Proceedings of the 22nd Photovoltaic Spec. Conference (IEEE, New York, 1991), p. 177.

3. F.S. Goucher, G.L. Pearson, M. Sparks, G.K. Teal, and W. Schockley, Phys. Rev., **81**, 637 (1951).

4. D.E. Newbury, D.C. Joy, P. Echlin, C.E. Fiori and J.I. Goldstein, Advanced Scanning Electron Microscopy and X-Ray Microanalysis (Plenum, New York, 1986), p. 65.

5. R.P. Leon, Proceedings of the 19th Photovoltaic Spec. Conference (IEEE, New York, 1987), p. 808.

6. W. van Roosbroeck, J. Appl. Phys., **26**, 380 (1955).

7. C. Hu and C. Drowley, Solid State Electron., **21**, 965 (1978).

8. J.F. Bresse, in Proceedings of the 5th Ann. SEM Symposium IITRI, edited by O. Johary and I. Corvin (IIT Research Institute, Chicago, 1972), pp. 105-112.

9. F. Berz and H.K. Kuiken, Solid State Electron., **19**, 437 (1976).

10. C. van Opdorp, Phillips Res. Rept., **32**, 192 (1977).

11. T. Fuyuki, H. Matsunami and T. Tanaka, J. Phys. D:Appl. Phys., **13**, 1093 (1980); ibid **13**, 1503 (1980).

12. G. Oelgart, J. Fiddicke and R. Reulke, Phys. Status Solidi A, **66**, 283 (1981).

13. C. Donolato, Solid State Electron., **25**, 1077 (1982).

14. R. Hakimzadeh, H.J. Möller and S. Bailey, Proceedings of the 22nd Photovoltaic Spec. Conference (IEEE, New York, 1991), p. 335.

15. M. Watanabe, H.C. Gatos and G. Actor, in Proceedings of the International Symp. on Solar Energy, edited by J.B. Berkowitz and I.A Lesk (Electrochem. Soc. 1976), pp. 283-289.

16. J.I. Goldstein, D.E. Newbury, P. Echlin, D.C. Joy, C. Fiori, and E. Lifshin, Scanning Electron Microscopy and X-Ray Microanalysis (Plenum , New York, 1981), p. 1080.

17. G.A. Hungerfold and D.B. Holt, Microscopy of Semiconducting Materials, Conf. Series Nov. 87, eds A.G. Cullis and P. Augustus, Institute of Physics, Bristol, pp. 721-726.

18. M. Faur, M. Faur, P. Jenkins, M. Goradia, S. Bailey, D. Jayne, I. Weinberg and C. Goradia, Surface and Interface Analysis, **15**, 745 (1990).

19. C.L. Chiang, S. Wagner and A.A. Ballman, Mater. Lett. **1**, 145 (1983).

20. S. Adachi and H. Kawaguchi, J. Electrochem. Soc., **128**, 1342 (1981).

TABLE I. Measured values of L_n and s.

Wafer Number	Sample Number	L_n (μm)	Range of s ($x10^3$ cm^{-1})
3	1	0.64	37.42 - 47.71
3	2	1.36	8.86 - 64.87
3	5	0.78	4.25 - 19.28
3	7	0.39	5.74 - 33.61
3	8	0.45	87.25 - 108.33
3	13	0.44	52.73 - 135.03
3	14	0.77	149.52 - 183.08
2	19	0.26	88.71 - 347.23
2	20	0.38	154.08 - 171.57
2	21	0.36	136.76 - 164.21
2	23	0.26	33.17 - 51.47
2	25	0.39	8.50 - 52.12
2	26	0.73	17.16 - 36.93
2	28	0.34	36.18 - 109.68
2	30	0.50	53.43 - 71.73
2	31	0.39	91.50 - 143.46
2	32	0.50	116.02 - 186.98
2	33	0.78	137.09 - 149.02

All wafers had the following specifications:
Crystacomm crystal #4420, zinc-doped with a carrier concentration of 1×10^{18} cm^{-3}.

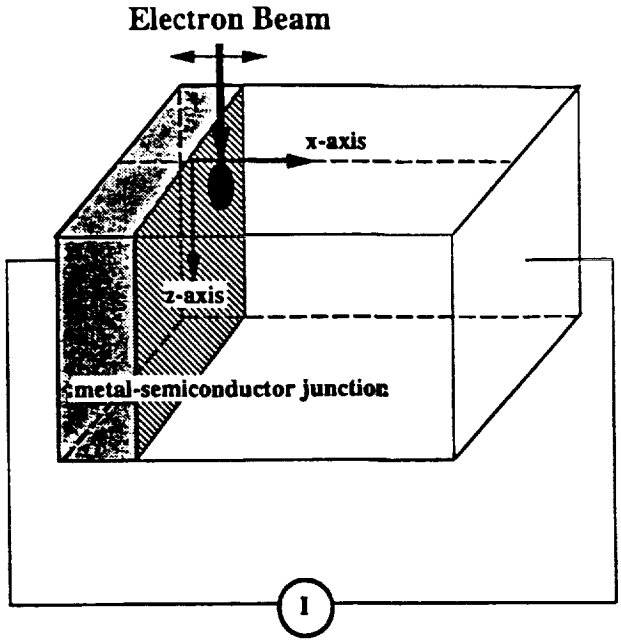

Figure 1. Schematic diagram of the beam-specimen interaction (normal collector geometry).

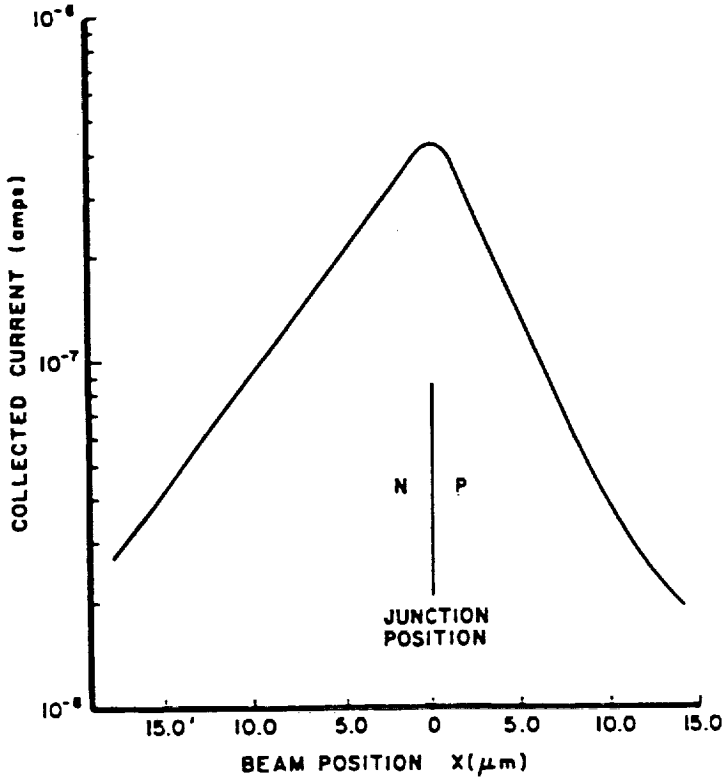

Figure 2. EBIC signal variations around a vertical p-n junction. (Reproduced from [4]).

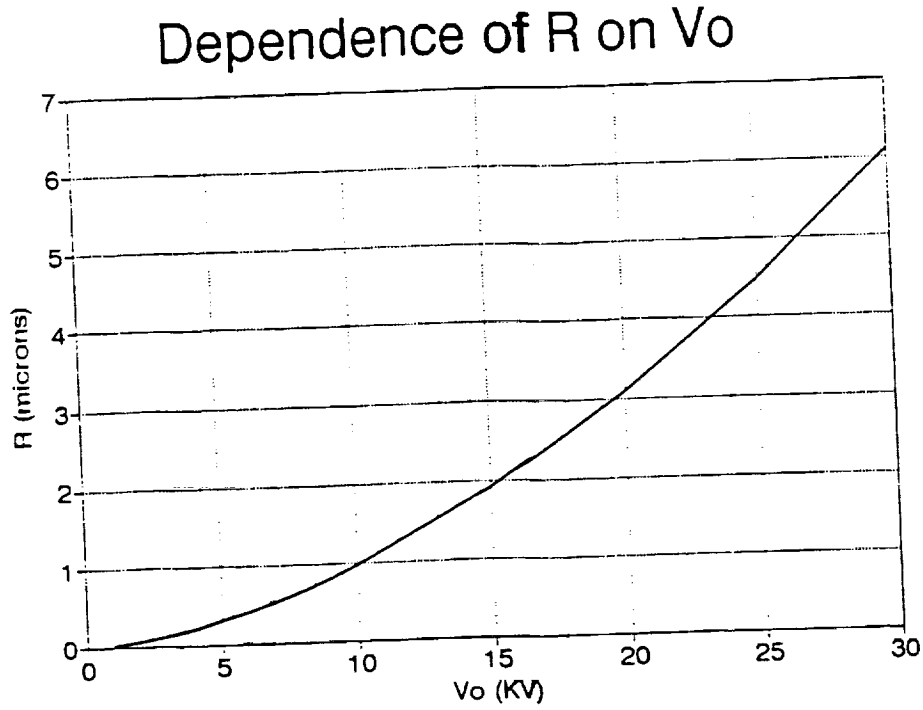

Figure 3. Plot of R as a function of V_o.

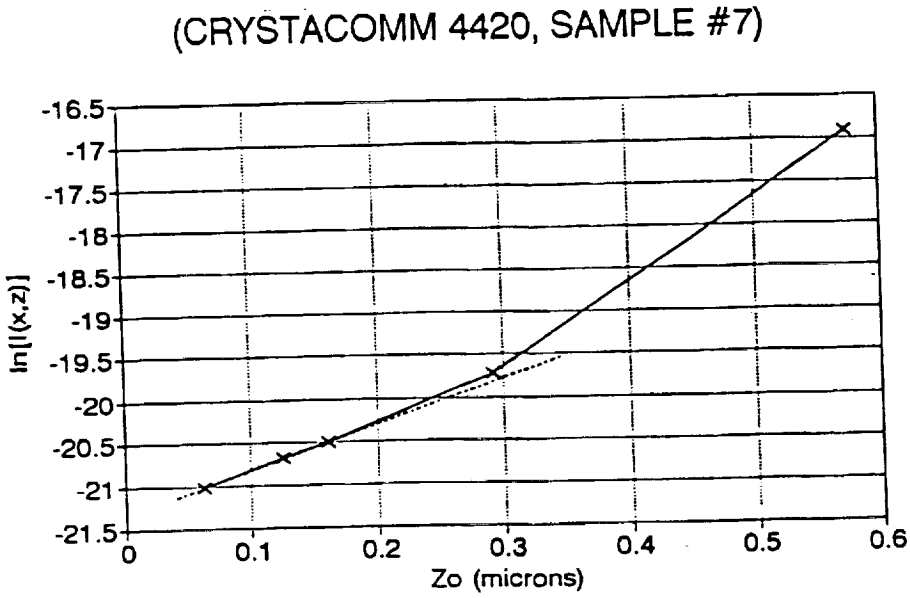

Figure 4. Plot of ln[I(x,z)] versus Z_o for a typical sample and for x = 0.52 μm.

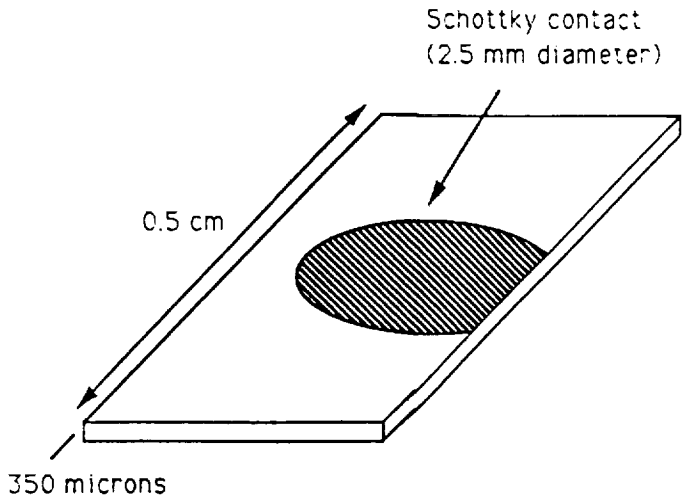

Figure 5. Schematic diagram of a cleaved InP Schottky specimen.

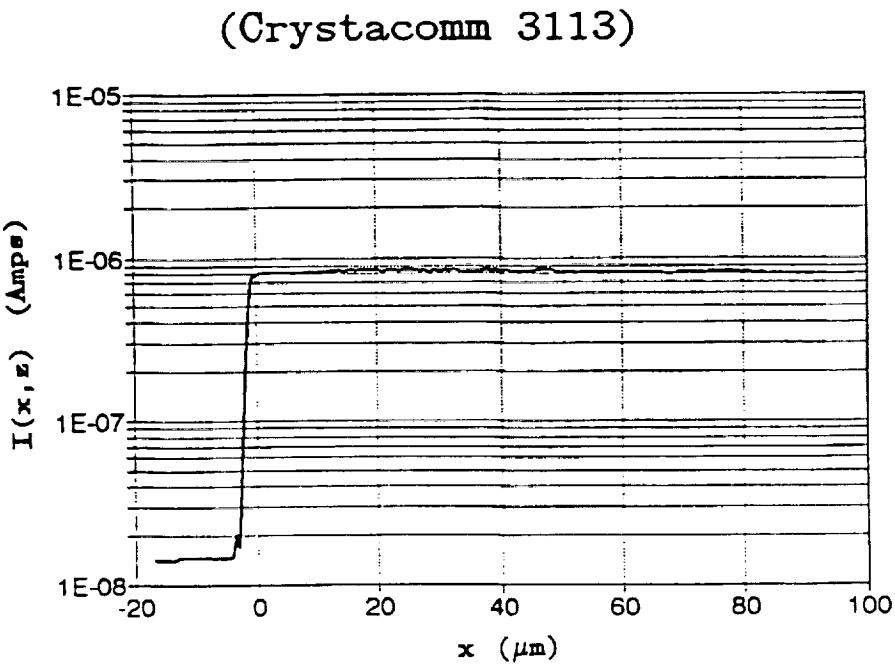

Figure 6. Typical EBIC profile of a specimen with dopant density = 2 x 10^{16} cm^{-3}.

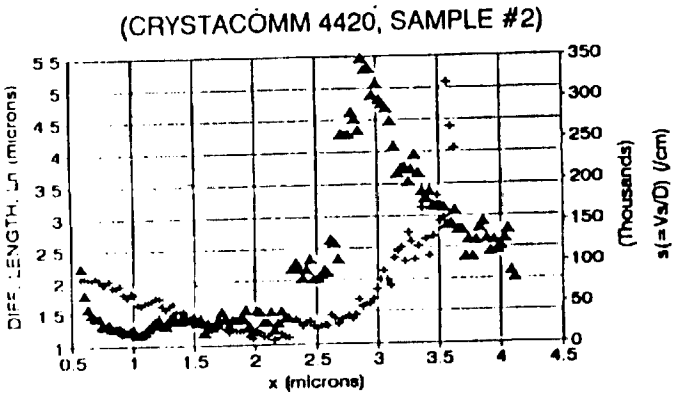

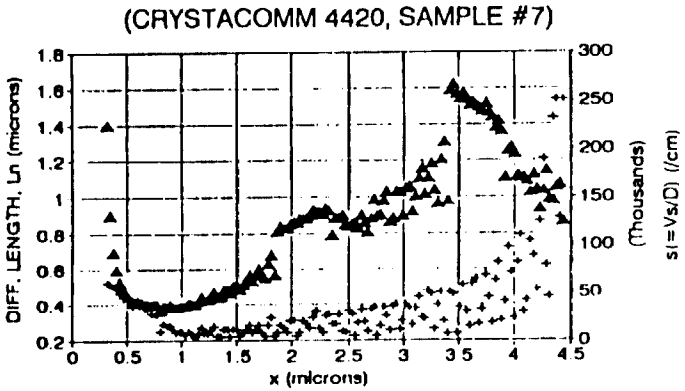

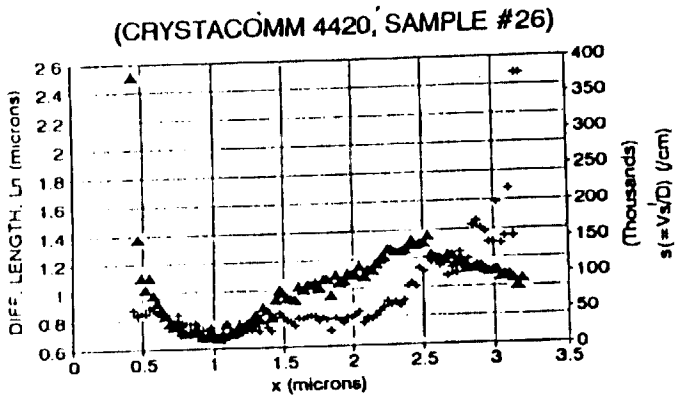

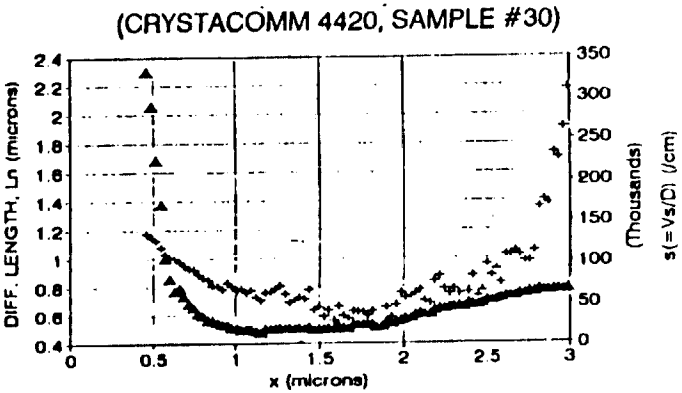

Figure 7. Results obtained for four typical samples. ▲ = L_n, + = s.

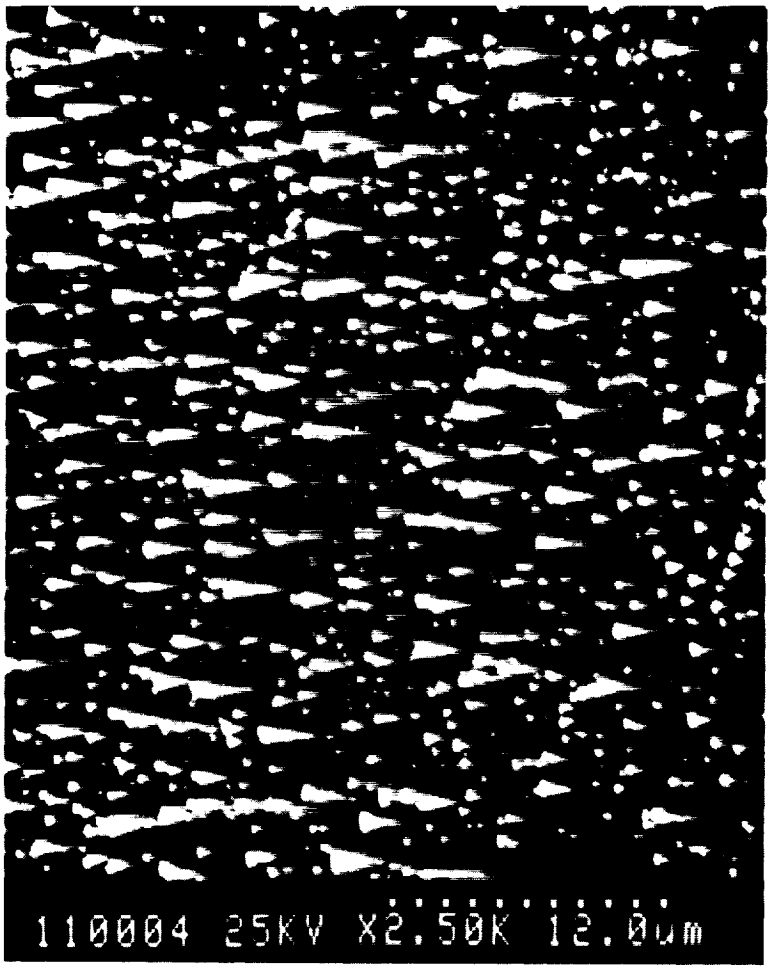

Figure 8. Photograph of a pitted surface, created by etching the edge surface in HCl.

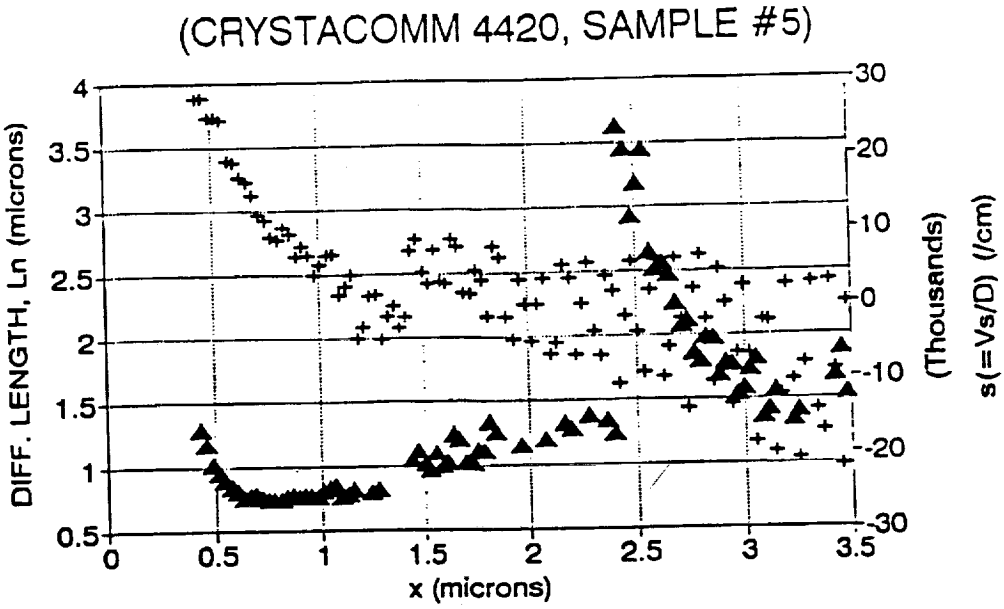

(a)

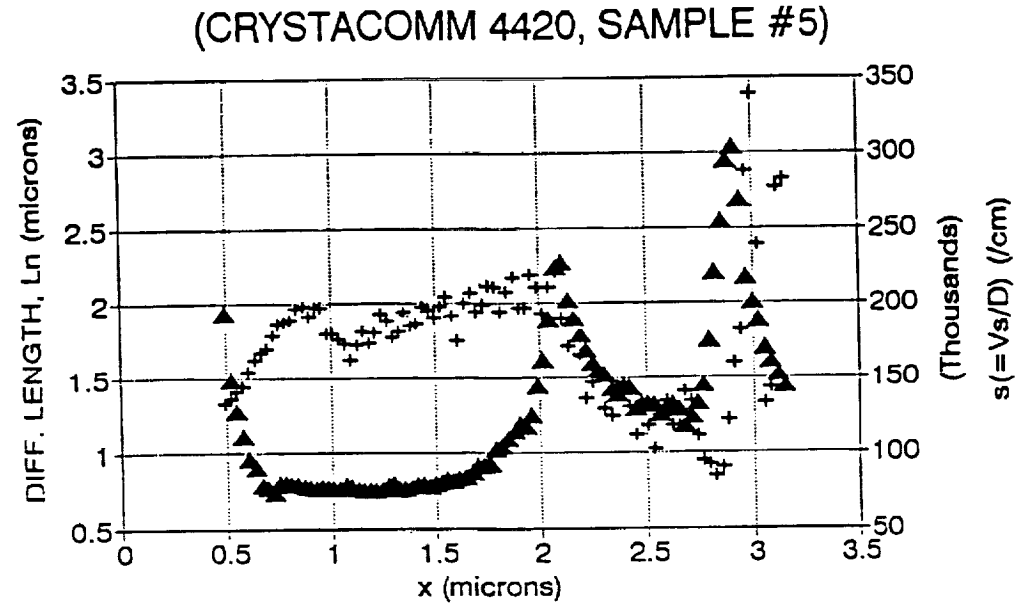

(b)

Figure 9. Results obtained in a typical specimen (a) before etching in HCl, (b) after etching in HCl.